nature immunology

The inflammasome adaptor ASC regulates the function of adaptive immune cells by controlling Dock2-mediated Rac activation and actin polymerization

Sirish K Ippagunta[1,7], R K Subbarao Malireddi[1,7], Patrick J Shaw[1,7], Geoffrey A Neale[2], Lieselotte Vande Walle[3,4], Douglas R Green[1], Yoshinori Fukui[5,6], Mohamed Lamkanfi[3,4] & Thirumala-Devi Kanneganti[1]

The adaptor ASC contributes to innate immunity through the assembly of inflammasome complexes that activate the cysteine protease caspase-1. Here we demonstrate that ASC has an inflammasome-independent, cell-intrinsic role in cells of the adaptive immune response. ASC-deficient mice showed defective antigen presentation by dendritic cells (DCs) and lymphocyte migration due to impaired actin polymerization mediated by the small GTPase Rac. Genome-wide analysis showed that ASC, but not the cytoplasmic receptor NLRP3 or caspase-1, controlled the mRNA stability and expression of Dock2, a guanine nucleotide–exchange factor that mediates Rac-dependent signaling in cells of the immune response. Dock2-deficient DCs showed defective antigen uptake similar to that of ASC-deficient cells. Ectopic expression of Dock2 in ASC-deficient cells restored Rac-mediated actin polymerization, antigen uptake and chemotaxis. Thus, ASC shapes adaptive immunity independently of inflammasomes by modulating Dock2-dependent Rac activation and actin polymerization in DCs and lymphocytes.

Inflammasomes are intracellular multiprotein complexes that are emerging as key regulators of the innate immune response. Deregulated inflammasome activity has been linked to autoimmune diseases, including inflammatory bowel diseases[1–5], vitiligo[6], gouty arthritis[7] and type I and type II diabetes[8,9] and less common autoinflammatory disorders collectively referred to as 'cryopyrinopathies'[10,11]. Distinct inflammasome complexes are assembled around members of the Nod-like receptor (NLR) family or DNA-binding HIN-200 family in a pathogen-specific manner[12–14]. NLRC4 assembles an inflammasome in macrophages infected with intracellular pathogens such as *Salmonella typhimurium*, *Legionella pneumophila*, *Pseudomonas aeruginosa* and *Shigella flexneri*[15–22]. In contrast, lethal toxin from *Bacillus anthracis* triggers activation of the NLRP1B inflammasome in mouse macrophages, and *Nlrp1b* has been identified as the key susceptibility locus for anthrax lethal toxin–induced macrophage death[23]. NLRP3 mediates activation of the cysteine protease caspase-1 in lipopolysaccharide (LPS)-primed macrophages that are exposed to microbial components with diverse molecular structures such as viral RNA and DNA or microbial toxins such as the ionophore nigericin[17,24–27]. In addition, the endogenous danger-associated molecules monosodium urate and calcium pyrophosphate dehydrate crystals also activate the NLRP3 inflammasome, which suggests a role for this inflammasome in the etiology of gouty arthritis and pseudogout[7]. The NLRP3 inflammasome contributes to host defense against *Salmonella* infection *in vivo*[28]. Moreover, published reports have characterized the critical role of the NLRP3 inflammasome in protection against colitis and colitis-associated tumorigenesis[2,3,5]. Finally, DNA viruses such as vaccinia virus and cytomegalovirus and the bacterial pathogens *Francisella tularensis* and *Listeria monocytogenes* induce activation of caspase-1 through the HIN-200 family member AIM2 (refs. 29–34). Once activated, caspase-1 cleaves and allows secretion of bioactive interleukin 1β (IL-1β) and IL-18. In addition, caspase-1 mediates a specialized form of cell death in infected macrophages and dendritic cells (DCs), a process that contributes substantially to the pathophysiology of several infectious diseases[12,35].

The adaptor ASC (Pycard) was initially believed to exert its effects on immune signaling mainly by bridging the interaction between NLRs or HIN-200 proteins and caspase-1 in inflammasome complexes[36,37]. However, emerging evidence has indicated important inflammasome-independent roles for ASC in controlling immune responses. For instance, the adjuvant quality of the oil-in-water emulsion MF59 has been shown to require ASC, whereas the inflammasome components NLRP3 and caspase-1 are dispensable[38]. Consequently, the induction of antigen-specific γ-immunoglobulin (IgG) antibodies to influenza vaccines in MF59 is impaired in mice that lack ASC (*Pycard*$^{-/-}$; called '*Asc*$^{-/-}$' here) but not in NLRP3-deficient (*Nlrp3*$^{-/-}$) mice or caspase-1-deficient (*Casp1*$^{-/-}$) mice[38]. Moreover, granuloma formation and host defense in chronic *Mycobacterium tuberculosis* infection depends

[1]Department of Immunology, St. Jude Children's Research Hospital, Memphis, Tennessee, USA. [2]Department of Hartwell Center for Bioinformatics & Biotechnology, St. Jude Children's Research Hospital, Memphis, Tennessee, USA. [3]Department of Biochemistry, Ghent University, Ghent, Belgium. [4]Department of Medical Protein Research, VIB, Ghent, Belgium. [5]Division of Immunogenetics, Kyushu University, Kyushu, Japan. [6]Department of Immunobiology and Neuroscience Medical Institute of Bioregulation, Kyushu University, Kyushu, Japan. [7]These authors contributed equally to this work. Correspondence should be addressed to M.L. (mohamed.lamkanfi@vib-ugent.be) or T.-D.K. (thirumala-devi.kanneganti@stjude.org).

Received 13 June; accepted 27 July; published online 4 September 2011; addendum published after print 1 June 2012; doi:10.1038/ni.2095

on ASC but not on NLRP3 or caspase-1 (ref. 39). Finally, *Asc*$^{-/-}$ mice, but not *Nlrp3*$^{-/-}$ mice or *Casp1*$^{-/-}$ mice, are substantially protected against disease progression in experimental models of rheumatoid arthritis and experimental autoimmune encephalomyelitis (EAE), respectively[40–42]. Those last studies have indicated the existence of cell-intrinsic roles for ASC in DC and lymphocyte populations. However, the molecular effector mechanism by which ASC regulates adaptive immune responses independently of inflammasomes has remained unclear.

Here we show that ASC has a critical cell-intrinsic role in regulating immune-cell functions in lymphocytes and DCs in an inflammasome-independent manner. The chemotaxis of *Asc*$^{-/-}$ lymphocytes, but not of *Nlrp3*$^{-/-}$ or *Casp1*$^{-/-}$ lymphocytes, was considerably impaired despite normal expression of chemokine receptors and downstream mitogen-activated protein kinase (MAPK) signaling. Instead, *Asc*$^{-/-}$ lymphocytes failed to migrate because of defective actin polymerization induced by the small GTPase Rac at the leading edge of leukocytes. Consequently, total lymphocyte and DC populations in secondary lymphoid organs were much smaller in *Asc*$^{-/-}$ mice but not in *Nlrp3*$^{-/-}$ or *Casp1*$^{-/-}$ mice. Rac activation and actin polymerization have a critical role in other cell type functions as well, including the uptake of antigens by DCs[43]. Accordingly, ASC-deficient DCs were impaired in their ability to take up antigens and to drive T cell proliferation. Again, inflammasome signaling was dispensable for ASC-mediated antigen presentation and T cell activation. Instead, transcriptome analysis showed that ASC specifically regulated the transcript abundance of Dock2, a guanine nucleotide–exchange factor specific for cells of the immune response that mediates Rac-dependent actin polymerization and migration of T cells and B cells[44]. As in *Asc*$^{-/-}$ cells, we identified a critical role for Dock2 in antigen uptake by DCs. Moreover, ectopic expression of Dock2 in *Asc*$^{-/-}$ lymphocytes and DCs restored ASC-dependent immune functions, which confirmed that Dock2 is the main effector that drives the inflammasome-independent functions of ASC in cells of the immune response. Thus, ASC regulates adaptive immune responses by controlling Dock2 expression in DCs and lymphocytes. Our results identify a previously unknown mechanism that regulates the function of cells of the adaptive immune response and provide a mechanistic explanation for the critical inflammasome-independent role of ASC in driving T cell and humoral responses after vaccination and in autoimmune disease.

RESULTS

Antigen uptake and presentation require ASC

The presentation of antigenic peptides on receptors for major histocompatibility complex class II of 'professional' phagocytes represents a critical step in the activation of adaptive immune responses that is dependent on actin polymerization[43]. We confirmed the critical role of ASC in antigen presentation by receptors for major histocompatibility complex class II with the observation that *Asc*$^{-/-}$ DCs were severely impaired in inducing the proliferation of bovine serum albumin (BSA)-specific T cells (**Fig. 1a**). Moreover, wild-type T cells incubated with *Asc*$^{-/-}$ DCs in the presence of BSA produced significantly lower amounts cytokines of the T helper type 1 (T_H1) subset (interferon-γ; **Fig. 1b**), the T_H2 subset (IL-6 and IL-10; **Fig. 1c** and **Supplementary Fig. 1**) and the T_H17 subset of helper T cells (IL-17; **Fig. 1d**), which further established the critical role for ASC in priming T cells. Unlike *Asc*$^{-/-}$ DCs, *Nlrp3*$^{-/-}$ DCs and *Casp1*$^{-/-}$ DCs elicited a T cell–proliferative response similar to that induced by wild-type DCs (data not shown), which emphasizes the role of ASC in antigen presentation by DCs that is independent of its role in inflammasome activation.

The recognition and uptake of antigen by professional antigen-presenting cells represents one of the first steps in presenting peptides to receptors for major histocompatibility class II (ref. 43). To explore the possibility that ASC is required for antigen uptake by professional phagocytes, we incubated wild-type, *Nlrp3*$^{-/-}$, *Asc*$^{-/-}$ and *Casp1*$^{-/-}$ bone marrow–derived DCs (BMDCs) for 3 h with fluorescein isothiocyanate (FITC)-labeled zymosan A or polystyrene beads and measured phagocytosis by flow cytometry. Internalization of zymosan A or polystyrene beads by *Asc*$^{-/-}$ BMDCs was impaired, whereas phagocytosis by *Nlrp3*$^{-/-}$ and *Casp1*$^{-/-}$ BMDCs was similar to that of wild-type cells (**Fig. 1e**). This result confirmed that *Asc*$^{-/-}$ BMDCs were defective in the phagocytosis of particulate antigens. To determine whether the uptake of small soluble antigens, which proceeds via fluid endocytosis (macropinosis), was also affected by ASC deficiency, we incubated wild-type, *Nlrp3*$^{-/-}$, *Asc*$^{-/-}$ and *Casp1*$^{-/-}$ BMDCs for 3 h with FITC-labeled dextran, FITC-labeled ovalbumin (OVA) or lucifer yellow, then washed the cells and assessed macropinosis of these substances by flow cytometry. *Asc*$^{-/-}$ DCs were defective in internalizing all three; in contrast, macropinosis of these by *Nlrp3*$^{-/-}$ and *Casp1*$^{-/-}$ BMDCs was not affected (**Fig. 1f**). Together these results indicate that ASC controls the uptake and presentation of antigens in professional antigen-presenting cells independently of inflammasomes.

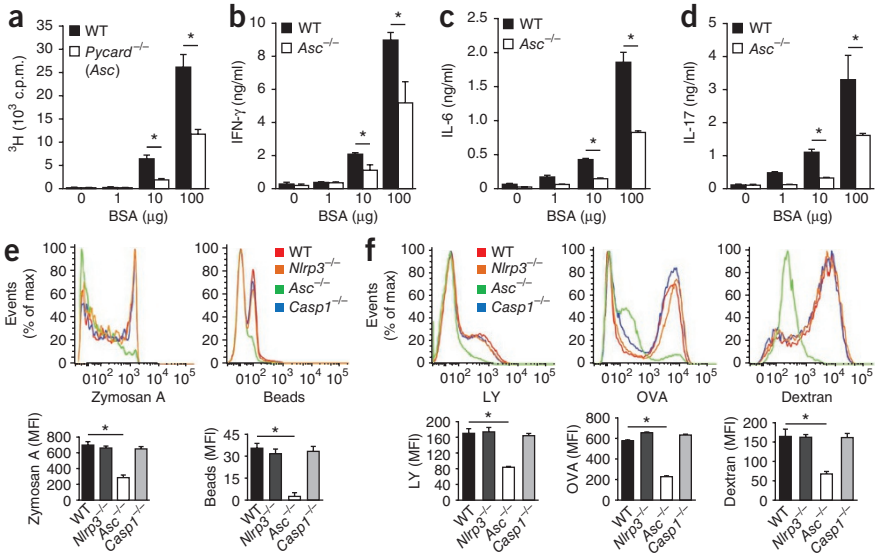

Figure 1 ASC controls antigen uptake and presentation independently of inflammasomes. (**a**–**d**) Dose-dependent antigen-specific proliferation of lymphocytes among DCs obtained from naive wild-type (WT) and *Asc*$^{-/-}$ mice ($n = 4$–6 per group) and cultured for 72 h with wild-type CD4$^+$ T cells in the presence of 0–100 μg BSA, assessed as uptake of [^{3}H]thymidine (**a**) and as the concentration of interferon-γ (IFN-γ; **b**), IL-6 (**c**) and IL-17 (**d**). *$P < 0.01$ (two-tailed Student's *t*-test). (**e**) Flow cytometry analysis of the phagocytosis of fluorescein-labeled zymosan A or polystyrene beads by wild-type, *Nlrp3*$^{-/-}$, *Asc*$^{-/-}$ and *Casp1*$^{-/-}$ BMDCs after incubation together for 3 h at 37 °C. MFI, mean fluorescence intensity. *$P < 0.0005$ (two-tailed Student's *t*-test). (**f**) Flow cytometry analysis of the macropinocytosis of fluorescein-labeled luciferase yellow (LY), OVA or dextran by wild-type, *Nlrp3*$^{-/-}$, *Asc*$^{-/-}$ and *Casp1*$^{-/-}$ BMDCs after incubation as in **e**. *$P < 0.005$ (two-tailed Student's *t*-test). Data are representative of three independent experiments (**a**–**d**; mean and s.d.) or at least three independent experiments (**e**,**f**; mean and s.e.m. of triplicates).

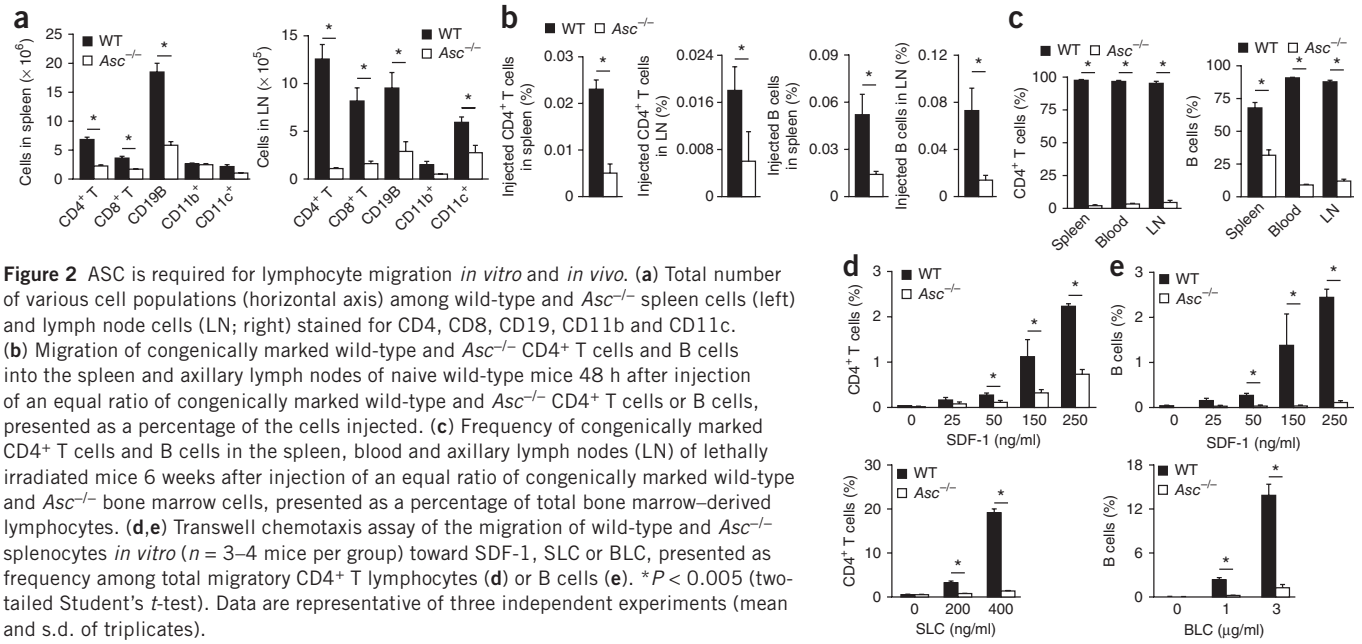

Figure 2 ASC is required for lymphocyte migration *in vitro* and *in vivo*. (**a**) Total number of various cell populations (horizontal axis) among wild-type and *Asc*$^{-/-}$ spleen cells (left) and lymph node cells (LN; right) stained for CD4, CD8, CD19, CD11b and CD11c. (**b**) Migration of congenically marked wild-type and *Asc*$^{-/-}$ CD4$^+$ T cells and B cells into the spleen and axillary lymph nodes of naive wild-type mice 48 h after injection of an equal ratio of congenically marked wild-type and *Asc*$^{-/-}$ CD4$^+$ T cells or B cells, presented as a percentage of the cells injected. (**c**) Frequency of congenically marked CD4$^+$ T cells and B cells in the spleen, blood and axillary lymph nodes (LN) of lethally irradiated mice 6 weeks after injection of an equal ratio of congenically marked wild-type and *Asc*$^{-/-}$ bone marrow cells, presented as a percentage of total bone marrow–derived lymphocytes. (**d**,**e**) Transwell chemotaxis assay of the migration of wild-type and *Asc*$^{-/-}$ splenocytes *in vitro* (n = 3–4 mice per group) toward SDF-1, SLC or BLC, presented as frequency among total migratory CD4$^+$ T lymphocytes (**d**) or B cells (**e**). *$P < 0.005$ (two-tailed Student's t-test). Data are representative of three independent experiments (mean and s.d. of triplicates).

ASC is critical for lymphocyte chemotaxis and migration

In addition to its role in regulating antigen uptake by professional phagocytes, ASC has been proposed to exert cell-intrinsic functions in lymphocytes[41,42]. In agreement with that, the total number of spleen and lymph node cells in *Asc*$^{-/-}$ mice was about half of that in wild-type mice, with counts of CD4$^+$ T cells, CD8$^+$ T cells, B cells and CD11c$^+$ cells all much lower in *Asc*$^{-/-}$ spleens and lymph nodes (**Fig. 2a**). *Nlrp3*$^{-/-}$ and *Casp1*$^{-/-}$ mice had numbers similar to those of wild-type mice in both the spleen and lymph nodes for each cell population (**Supplementary Fig. 2**). To determine whether ASC has an important role during lymphocyte migration and T cell development, we analyzed the migration of congenically marked wild-type and *Asc*$^{-/-}$ lymphocytes to peripheral lymph nodes and spleens of wild-type mice. The intrinsic migratory ability of *Asc*$^{-/-}$ T cells and B cells was impaired, as indicated by the significantly lower number of both cell types retrieved from the spleen and lymph nodes of wild-type hosts (**Fig. 2b**). To confirm the intrinsic migratory defect of *Asc*$^{-/-}$ lymphocytes, we created mixed chimeras by injecting an equal ratio of wild-type and *Asc*$^{-/-}$ bone marrow into lethally irradiated wild-type mice. At 6 weeks after reconstitution, ~98% of the CD4$^+$ T cells found in blood and secondary lymphoid organs were derived from wild-type bone marrow (**Fig. 2c**). Similarly, most circulating B cells were wild-type cells (**Fig. 2c**). In addition to being the result of intrinsic defects in migration, the very high ratio of wild-type lymphocytes to *Asc*$^{-/-}$ lymphocytes in mixed chimeras could also have been due to differences in lymphocyte development and cell survival. Although leukocyte populations in *Asc*$^{-/-}$ mice (**Supplementary Fig. 3**) and chimera mice with *Asc*$^{-/-}$ bone marrow (**Supplementary Fig. 4**) indeed contained slightly fewer single-positive (CD4$^+$ or CD8$^+$) thymocytes and modestly more double-negative (CD4$^-$CD8$^-$) T cells, these differences in thymocyte development were only minor. Nevertheless, to further confirm the migratory phenotype of *Asc*$^{-/-}$ T cells and B cells, we studied the *in vitro* migration of these cells toward chemokines. In agreement with a critical role for ASC in lymphocyte chemotaxis, splenic CD4$^+$ T cells from *Asc*$^{-/-}$ mice were nearly completely unable to migrate toward the chemokines SDF-1 and SLC (**Fig. 2d**). Similarly, B cells from *Asc*$^{-/-}$ mice were defective in their migration toward both SDF-1 and the lymphocyte chemokine BLC (**Fig. 2e**). In contrast, splenic T lymphocytes and B lymphocytes of *Nlrp3*$^{-/-}$ and *Casp1*$^{-/-}$ mice migrated toward these chemokines to a degree similar to that of wild-type lymphocytes (**Supplementary Fig. 5**). Thus, ASC is required for lymphocyte migration *in vitro* and *in vivo*.

ASC controls Rac activation and actin polymerization

Both efficient endocytosis of antigens and the migration of lymphocytes toward a chemokine gradient require the activation of small GTPases such as Cdc42 and Rac to induce F-actin polymerization and cytoskeletal reorganization[43]. However, the expression and activation of Cdc42 were not altered in *Asc*$^{-/-}$ BMDCs and lymphocytes, respectively (**Supplementary Fig. 6**). In contrast, *Asc*$^{-/-}$ BMDCs were impaired in Rac activation (**Fig. 3a**) and F-actin polymerization (**Fig. 3b**) when incubated with OVA. Because lymphocyte migration relies on Rac activation and actin polymerization induced by chemokine receptors, we assessed the extent of Rac activation after chemokine stimulation. Although wild-type CD4$^+$ T cells and B cells activated Rac (**Fig. 3c**) and induced F-actin polymerization (**Fig. 3d**) after incubation with SDF-1 (500 ng/ml), these responses were much lower in *Asc*$^{-/-}$ T cells and B cells (**Fig. 3c**,**d**). The role of ASC in Rac activation and F-actin polymerization induced by chemokines in lymphocytes was specific, because SDF-1-induced activation of the MAPK Erk was not affected in *Asc*$^{-/-}$ T lymphocytes and B lymphocytes (**Supplementary Fig. 7**). Thus, defective antigen uptake by *Asc*$^{-/-}$ DCs and chemotaxis of *Asc*$^{-/-}$ lymphocytes is linked to impaired Rac activation and F-actin polymerization in these cells.

ASC regulates Dock2 expression independently of inflammasomes

Our results showed that ASC regulates antigen uptake in DCs and the migration of lymphocytes independently of inflammasomes through the modulation of Rac activation and F-actin polymerization. To characterize the molecular mechanism involved, we did microarray experiments to identify genes dysregulated in *Asc*$^{-/-}$ BMDCs despite their normal expression in *Nlrp3*$^{-/-}$ or *Casp1*$^{-/-}$ cells. Notably, among the more than 39,000 transcripts present on the microarray, the transcripts of only 5 genes were downregulated at least 66% in *Asc*$^{-/-}$ BMDCs relative to their expression in wild-type BMDCs (**Fig. 4a**). In addition to *Asc*, these included *Dock2* (80%) and the genes encoding follistatin-like 1 protein (*Fstl1*; 80%), galanin (*Gal*; 73%) and fatty acid–binding

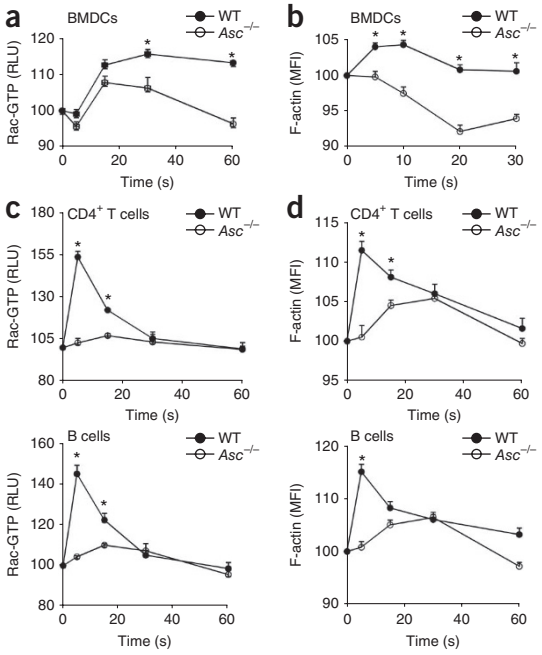

Figure 3 ASC is essential for Rac activation and actin polymerization, induced by antigens or chemokines in DCs or lymphocytes, respectively. (**a**,**b**) Flow cytometry analysis of Rac GTPase activity (**a**) and F-actin polymerization (**b**) in wild-type and *Asc*$^{-/-}$ BMDCs treated for 0–60 s (**a**) or 0–30 s (**b**) with OVA, presented as relative light units (RLU; **a**) or mean fluorescence intensity (**b**) relative to baseline, set as 100. (**c**) Small G protein–activation assay of Rac activation in lysates of CD4$^+$ T cells and B cells isolated from spleens of wild-type and *Asc*$^{-/-}$ mice and treated for 0–60 s *in vitro* with SDF-1 (500 ng/ml). (**d**) Flow cytometry analysis of F-actin polymerization in CD4$^+$ T cells and B cells isolated from wild-type and *Asc*$^{-/-}$ mice (n = 1–3 per group) and treated for 0–60 s *in vitro* with SDF-1 (500 ng/ml). *P <0.05 (two-tailed Student's t-test). Data are representative of at least three independent experiments (mean and s.d. of triplicates).

protein 4 (*Fabp4*; 70%). Quantitative PCR analysis confirmed the lower expression of *Dock2* mRNA in *Asc*$^{-/-}$ BMDCs (**Fig. 4b**), but the expression of *Fstl1*, *Gal* and *Fabp4* was unaltered in *Asc*$^{-/-}$ BMDCs (data not shown). Unlike *Asc*$^{-/-}$ BMDCs, *Nlrp3*$^{-/-}$ and *Casp1*$^{-/-}$ BMDCs had normal abundance of *Dock2* mRNA (**Fig. 4b**), which confirmed that *Dock2* transcript abundance is regulated by ASC in an inflammasome-independent manner. We observed similarly lower *Dock2* transcript abundance in the absence of ASC in CD4$^+$ T cells and isolated B cells (**Fig. 4c**). In contrast, *Dock2* mRNA expression in *Nlrp3*$^{-/-}$ and *Casp1*$^{-/-}$ CD4$^+$ T cells and B cells was similar to that of wild-type cells (data not shown).

We next prepared lysates of wild-type, *Nlrp3*$^{-/-}$, *Asc*$^{-/-}$ and *Casp1*$^{-/-}$ BMDCs to assess the expression of Dock2, FSTL1, FABP4 and galanin by immunoblot analysis. Notably, Dock2 expression was nearly abolished in *Asc*$^{-/-}$ BMDCs but was not altered in *Nlrp3*$^{-/-}$ and *Casp1*$^{-/-}$ BMDCs (**Fig. 4d**). The expression of FSTL1, galanin and FABP4 was not altered in *Asc*$^{-/-}$ BMDCs (**Fig. 4d**), which confirmed the results of quantitative PCR. Additionally, activation of the NLRP3 inflammasome by stimulation with LPS and ATP did not upregulate Dock2 expression in *Asc*$^{-/-}$ BMDCs or macrophages (**Supplementary Fig. 8**). Moreover, Dock2 expression remained stable in *Nlrp3*$^{-/-}$ and *Casp1*$^{-/-}$ BMDCs treated with those stimuli (**Supplementary Fig 8**). We confirmed ASC-dependent Dock2 expression in the BMDMs used above and BMDCs from an independently generated line of ASC-deficient mice[45] (**Supplementary Fig. 9**). We also observed the nearly complete absence of Dock2 protein in *Asc*$^{-/-}$ T cells and B cells (**Fig. 4e**). These results indicate that ASC specifically regulates Dock2 expression in an inflammasome-independent manner in myeloid cells and lymphocytes. We also explored whether ASC regulates Dock2 expression in a Toll-like receptor (TLR)-dependent way, but Dock2 expression was normal in BMDCs isolated from mice deficient in TLR2 or TLR4, as well as in cells lacking the common TLR adaptors MyD88 or TRIF (**Fig. 4f**). Thus, ASC specifically regulates Dock2 expression in myeloid cells and lymphocytes in a TLR- and inflammasome-independent way.

ASC regulates *Dock2* mRNA stability

To characterize the mechanism by which ASC regulates *Dock2* mRNA abundance, we first analyzed the subcellular localization of ASC in BMDCs by subcellular fractionation. Notably, we detected ASC in both the cytosolic and nuclear fractions of naive BMDCs (**Fig. 5a**). The subcellular localization of ASC to these compartments remained largely stable after stimulation with LPS and ATP (**Fig. 5a**). As expected, the antibody to ASC did not detect immunoreactive bands in lysates of *Asc*$^{-/-}$ BMDCs, which confirmed its specificity. Unlike ASC, caspase-1 was located exclusively in the cytosol of naive and BMDCs stimulated with LPS and ATP (**Fig. 5a**), which suggested that the nuclear pool of ASC is not recruited to inflammasome complexes. In agreement with that, analysis of confocal micrographs indicated that ASC and caspase-1 localized together in the

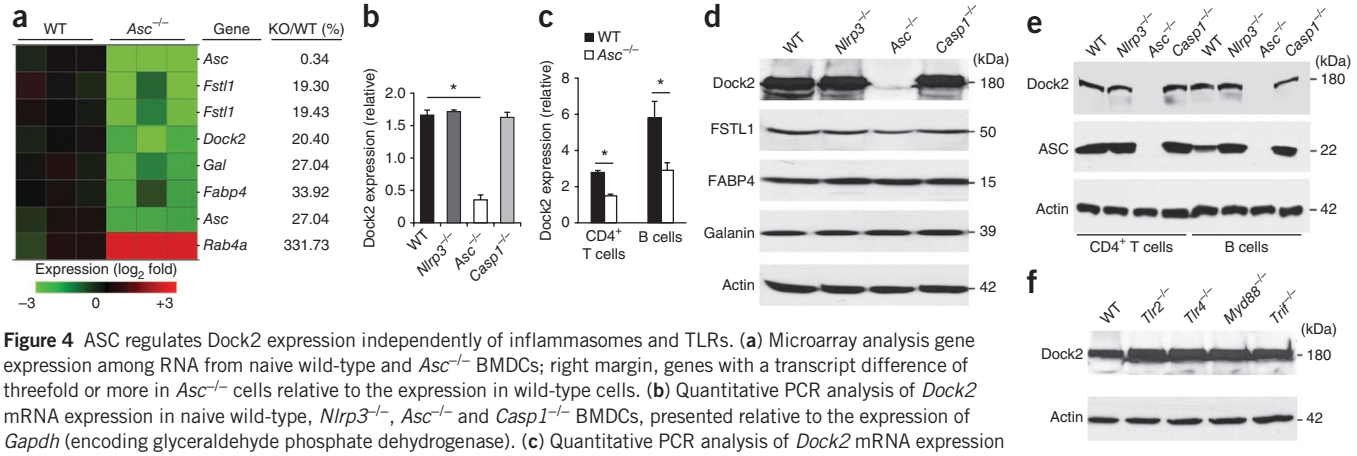

Figure 4 ASC regulates Dock2 expression independently of inflammasomes and TLRs. (**a**) Microarray analysis gene expression among RNA from naive wild-type and *Asc*$^{-/-}$ BMDCs; right margin, genes with a transcript difference of threefold or more in *Asc*$^{-/-}$ cells relative to the expression in wild-type cells. (**b**) Quantitative PCR analysis of *Dock2* mRNA expression in naive wild-type, *Nlrp3*$^{-/-}$, *Asc*$^{-/-}$ and *Casp1*$^{-/-}$ BMDCs, presented relative to the expression of *Gapdh* (encoding glyceraldehyde phosphate dehydrogenase). (**c**) Quantitative PCR analysis of *Dock2* mRNA expression in purified wild-type and *Asc*$^{-/-}$ CD4$^+$ T cells and B cells, presented as in **b**. (**d**) Immunoblot analysis of Dock2, FSTL1, FABP4 and galanin in naive wild-type, *Nlrp3*$^{-/-}$, *Asc*$^{-/-}$ and *Casp1*$^{-/-}$ BMDCs. kDa, kilodaltons. (**e**) Immunoblot analysis of Dock2 and ASC in purified wild-type, *Nlrp3*$^{-/-}$, *Asc*$^{-/-}$ and *Casp1*$^{-/-}$ CD4$^+$ T cells and B cells. (**f**) Immunoblot analysis of Dock2 in lysates of naive wild-type, *Tlr2*$^{-/-}$, *Tlr4*$^{-/-}$, *Myd88*$^{-/-}$ and *Trif*$^{-/-}$ BMDCs. Actin serves as a loading control throughout. *P < 0.005 (two-tailed Student's t-test). Data are representative of at least three independent experiments (mean and s.d. in **b**,**c**).

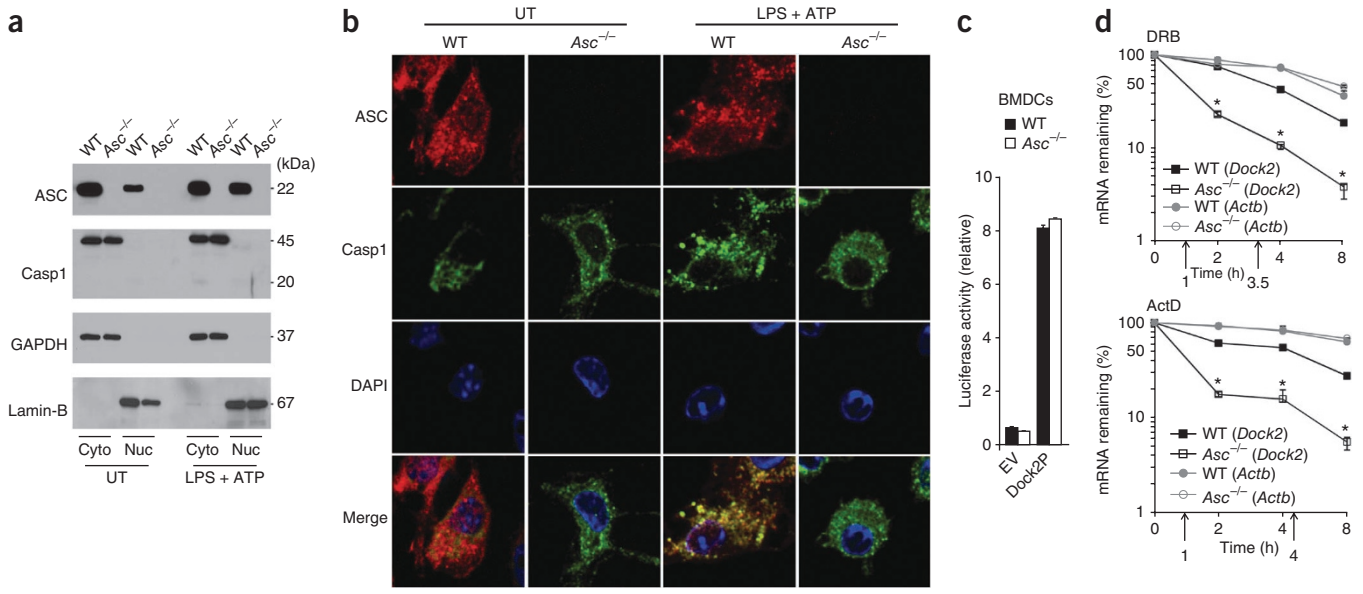

Figure 5 ASC localizes to the nucleus and controls the stability of *Dock2* mRNA. (**a**) Immunoblot analysis of ASC and caspase-1 (Casp1) in the cytosolic (Cyto) and nuclear (Nuc) compartments of wild-type and *Asc*$^{-/-}$ BMDCs left untreated (UT) or primed for 4 h with LPS (1 μg/ml), in the presence of ATP (5 mM) for the final 15 min (LPS + ATP). GAPDH and lamin-B serve as compartment-specific markers for the cytosolic and nuclear compartments, respectively. (**b**) Microscopy of wild-type and *Asc*$^{-/-}$ BMDCs left untreated or primed and treated as in **a**, then washed in PBS, fixed, made permeable and stained for ASC and caspase-1. The DNA-intercalating dye DAPI stains nuclei. Original magnification, ×63. (**c**) Luciferase activity of wild-type and *Asc*$^{-/-}$ BMDCs transfected by nucleofection with empty reporter vector (EV) or luciferase vector containing the *Dock2* promoter (Dock2P); results are presented relative to renilla luciferase activity. (**d**) Quantitative RT-PCR analysis of *Dock2* and *Actb* mRNA among total RNA from wild-type and *Asc*$^{-/-}$ BMDCs treated with DRB (50 μM) or actinomycin D (ActD; 5 μg/ml), normalized to the expression of *Gapdh* mRNA and presented relative to baseline expression, set as 100%; the half-life of mRNA (upward arrows) was calculated as the time required for decay to 50% of baseline. *$P < 0.005$ (Student's *t*-test). Data are representative of at least three independent experiments (mean and s.d. in **c**,**d**).

cytosol of BMDCs stimulated with LPS and ATP but not in untreated BMDCs (**Fig. 5b**). In contrast, ASC located in the nuclear compartment failed to localize together with caspase-1 under these conditions (**Fig. 5b**), which suggested that nuclear ASC may be responsible for regulating *Dock2* mRNA abundance in an inflammasome-independent manner.

We next assessed whether nuclear ASC regulated the transcriptional activity of the *Dock2* promoter. For this, we cloned the *Dock2* promoter into a luciferase reporter vector and used this to analyze *Dock2* promoter–driven luciferase production in wild-type and *Asc*$^{-/-}$ BMDCs. Luciferase expression was induced similarly in wild-type and *Asc*$^{-/-}$ BMDCs (**Fig. 5c**), which suggested that ASC may regulate *Dock2* mRNA abundance via mRNA stability instead. To investigate this possibility, we assessed *Dock2* mRNA stability in wild-type and *Asc*$^{-/-}$ BMDCs after treatment with the reversible transcription inhibitor DRB or actinomycin D to block new transcription. The half-life of *Dock2* transcripts was much lower in *Asc*$^{-/-}$ BMDCs (30 min) than in wild-type cells (~4 h; **Fig. 5d**). Unlike the half-life of *Dock2* mRNA, the half-life of *Actb* mRNA (encoding β-actin) was almost completely unaffected in *Asc*$^{-/-}$ BMDCs (**Fig. 5d**), which confirmed the specificity of these results. Thus, regulation of *Dock2* mRNA stability represents a major mechanism by which ASC controls Dock2 expression. To examine the potential contribution of post-translational events to the regulation of Dock2 expression, we pretreated wild-type and *Asc*$^{-/-}$ cells for 1, 4 or 6 h with the proteasome inhibitor MG132 before probing lysates for Dock2 expression. Proteasome inhibition resulted in slightly higher Dock2 expression in wild-type cells, but this was not sufficient to restore expression in *Asc*$^{-/-}$ cells (**Supplementary Fig. 10**).

Dock2 is critical for antigen uptake by DCs

Dock2 is member of a conserved family of guanine nucleotide–exchange factors that is specific to cells of the immune response and has been identified as a central regulator of the migration of lymphocytes and plasmacytoid DCs that controls Rac-dependent actin polymerization and cytoskeletal reorganization in these cells[44,46,47]. However, its role in DC function has not been characterized. We hypothesized that similar to *Asc*$^{-/-}$ BMDCs (**Fig. 1**), professional phagocytes lacking Dock2 might be impaired in antigen uptake and endocytosis. We first examined the macropinosis of FITC-labeled dextran, FITC-OVA and lucifer yellow by wild-type and *Dock2*$^{-/-}$ BMDCs. The uptake of dextran (**Fig. 6a**), OVA (**Fig. 6b**) and lucifer yellow (**Fig. 6c**) by *Dock2*$^{-/-}$ BMDCs was significantly impaired relative to their uptake by wild-type BMDCs, which indicated the importance of Dock2 in the endocytosis of soluble antigens by professional phagocytes. The uptake of larger particles and insoluble antigens proceeds through phagocytosis rather than macropinosis[48]. To determine the role of Dock2 in phagocytosis, we compared the uptake of FITC-labeled zymosan A and FITC-labeled polystyrene beads by wild-type and *Dock2*$^{-/-}$ BMDCs. In agreement with an important role for Dock2 in phagocytosis, *Dock2*$^{-/-}$ DCs were impaired in the internalization of zymosan A (**Fig. 6d**) and polystyrene beads (**Fig. 6e**) relative to the internalization of these by wild-type control cells. Notably, ASC expression and inflammasome activation were normal in *Dock2*$^{-/-}$ BMDCs (**Supplementary Fig. 11**), which further confirmed that ASC- and Dock2-mediated endocytosis is uncoupled from inflammasome signaling.

Ectopic expression of Dock2 restores ASC-mediated functions

The observation that Dock2 was critical for the internalization of soluble and insoluble antigens via both macropinosis and phagocytosis by professional antigen-presenting cells, together with our results showing that ASC controlled Dock2 expression in BMDCs and lymphocytes (**Figs. 4** and **5**), suggested that ASC may act upstream of

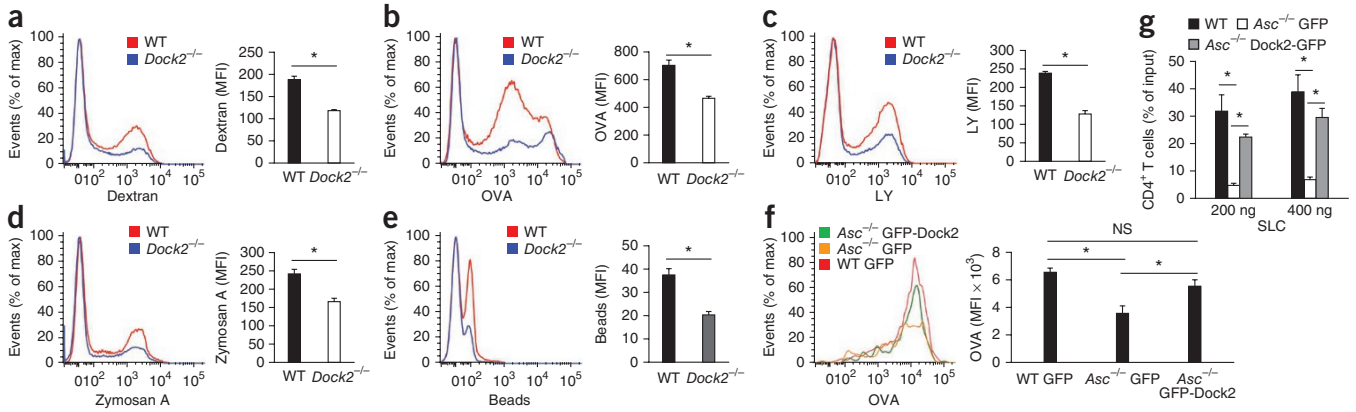

Figure 6 Dock2 is critical for antigen uptake by DCs and restores immune-cell functions in the absence of ASC. (**a**–**c**) Macropinocytosis of FITC-labeled dextran (**a**), OVA (**b**) or lucifer yellow (**c**) by wild-type and *Dock2*$^{-/-}$ BMDCs after incubation together for 3 h at 37 °C. (**d**–**e**) Phagocytosis of fluorescein-labeled zymosan A (**d**) or polystyrene beads (**e**) by wild-type and *Dock2*$^{-/-}$ BMDCs after incubation as in **a**. (**f**) Macropinocytosis of fluorescein-labeled OVA by wild-type and *Asc*$^{-/-}$ BMDCs transfected by nucleofection with plasmid expressing GFP or GFP-Dock2, assessed by flow cytometry 24 h after transfection. (**g**) Transwell chemotaxis assay of the *in vitro* migration of wild-type and *Asc*$^{-/-}$ CD4^{+} T lymphocytes expressing either GFP or GFP-Dock2 toward SLC; results are presented as the frequency among the total migrating T cell population. NS, not significant; $^{*}P < 0.05$ (two-tailed Student's *t*-test). Data are representative of at least three independent experiments (**a**–**g**; mean and s.e.m. of triplicates).

Dock2 in controlling Dock2-dependent immune functions. Therefore, we assessed whether the defective Rac activation, actin polymerization and antigen uptake by *Asc*$^{-/-}$ BMDCs and impaired migration of *Asc*$^{-/-}$ lymphocytes was due to the specific downregulation of *Dock2* in these cells. For this, we transfected *Asc*$^{-/-}$ BMDCs by nucleofection with plasmid encoding green fluorescent protein (GFP) alone or a GFP-Dock2 fusion protein. Endocytosis of OVA by *Asc*$^{-/-}$ BMDCs expressing GFP-Dock2 was significantly higher than its uptake by *Asc*$^{-/-}$ BMDCs expressing GFP alone (**Fig. 6f**), which confirmed the requirement for Dock2 downstream of ASC for antigen uptake by professional phagocytes. Similarly, ectopic expression of Dock2 in *Asc*$^{-/-}$ T cells restored their migration toward the chemokine SLC (**Fig. 6g**). Collectively, these data show that the functional defects of *Asc*$^{-/-}$ BMDCs and lymphocytes were due to a specific decrease in *Dock2* mRNA stability that led to impaired Dock2 expression in the absence of ASC and that ectopic expression of Dock2 in the cells was sufficient to restore ASC-dependent immune-cell functions.

DISCUSSION

The adaptor ASC is well known to contribute to innate immune responses by enabling activation of the cysteine protease caspase-1 in inflammasomes[45,49]. Studies have provided evidence indicating that *Asc*$^{-/-}$ mice are protected from disease progression in animal models of arthritis and multiple sclerosis, whereas mice lacking the inflammasome components NLRP3 or caspase-1 are not[40–42]. ASC has been suggested to affect the immune-cell functions of lymphocytes[41,42] and DCs[40]. Although such observations suggest that ASC controls immune-cell functions through inflammasome-independent mechanisms, the molecular pathways involved have remained unclear. ASC has been reported to regulate the activation of MAPKs in macrophages by interacting with the phosphatase DUSP10 in response to TLR ligands and infection with bacterial pathogens[50]. However, this function may be stimulus dependent, as earlier reports did not observe differences in MAPK signaling in activated and infected *Asc*$^{-/-}$ macrophages[45]. Furthermore, we failed to detect changes in chemokine-induced phosphorylation of Erk in *Asc*$^{-/-}$ cells of the immune response.

Instead, we found that antigen presentation by DCs and the migration of T lymphocytes and B lymphocytes were considerably diminished in *Asc*$^{-/-}$ mice as a result of impaired Rac-mediated actin polymerization. Microarray and immunoblot analysis of naive and stimulated *Asc*$^{-/-}$ DCs and lymphocytes showed that ASC specifically regulated Dock2 expression. The role of ASC in regulating the abundance of *Dock2* mRNA was highly specific, as only 5 transcripts of the 39,000 transcripts analyzed were up- or downregulated by at least 66% in *Asc*$^{-/-}$ BMDCs relative to their expression in wild-type BMDCs. Moreover, *Dock2* was the only ASC-regulated gene whose expression was altered at the protein level as well. Instead of directly affecting *Dock2* promoter activity, ASC had a critical role in stabilizing *Dock2* mRNA, as the half-life of *Dock2* transcripts was much lower (87.5%) in *Asc*$^{-/-}$ DCs. Further analysis is needed to determine the specific contribution of the nuclear and cytosolic pools of ASC to this process. Given that ASC lacks intrinsic enzymatic activity, ASC most probably affects Dock2 abundance by assembling one or more protein complex(es) in the cytosol and/or nucleus, distinct from the inflammasomes. Moreover, in addition to regulating the decay rate of *Dock2* transcripts, ASC may contribute to as-yet-unknown processes that regulate *Dock2* mRNA and Dock2 protein at the post-transcriptional and/or post-translational level. These may include microRNAs that target Dock2, splicing of *Dock2* mRNA linked to nonsense-mediated mRNA decay, trafficking of *Dock2* mRNA, the rate of Dock2 translation and the degree of post-translational modification that may influence the trafficking and degradation of Dock2 in lysosomes. However, the notable effect of ASC deficiency on the decay rate of *Dock2* mRNA may hamper detailed analysis of the potential role of ASC in regulating Dock2 expression through these additional mechanisms. Regardless of what proves to be true, we confirmed downregulated Dock2 expression as the mechanism that drove the defective phagocytosis and antigen presentation by DCs and dysfunctional chemotaxis of lymphocytes in the absence of ASC. For example, ectopic expression of Dock2 in ASC-deficient cells restored lymphocyte migration and antigen uptake by DCs. Thus, the observation that ASC controlled Dock2 expression and Dock2-mediated regulation of Rac activation and actin polymerization provides a molecular basis for the defective antigen presentation by DCs and the lymphocyte-intrinsic defects in cell migration observed in the studies cited above.

In conclusion, we have provided genetic evidence of a critical and unexpected role for ASC in regulating the motility of T lymphocytes and B lymphocytes and antigen uptake by professional antigen-presenting

cells independently of inflammasomes. Instead, ASC controlled the stability of *Dock2* transcripts and expression of Dock2. Our observations identify a previously unknown role for ASC in regulating adaptive immune responses that is intrinsic to lymphocytes and DCs. The vital role of ASC in regulating both adaptive and innate immune responses suggests that modulating ASC expression and function may represent a powerful therapeutic strategy for the treatment of inflammatory and autoimmune disorders.

METHODS

Methods and any associated references are available in the online version of the paper at http://www.nature.com/natureimmunology/.

Accession codes. GEO: microarray data, GSE30769.

Note: Supplementary information is available on the Nature Immunology website.

ACKNOWLEDGMENTS

We thank R. Flavell (Yale University School of Medicine), G. Nunez (University of Michigan) and S. Akira (Osaka University) for mutant mice; P. Vandenabeele (Ghent University) for anti-caspase-1; and H. Chi (St. Jude Children's Research Hospital) for retroviral plasmids and mutant mice. Supported by the US National Institutes of Health (R01AR056296 and R21AI088177 to T.-D.K.), the American Lebanese Syrian Associated Charities (T.-D.K.), the European Union Framework Program 7 (Marie-Curie grant 256432 to M.L.) and the Fund for Scientific Research-Flanders (M.L. and L.V.W.).

AUTHOR CONTRIBUTIONS

T.-D.K., M.L., S.K.I., P.J.S. and R.K.S.M. designed research; S.K.I., P.J.S., R.K.S.M., did research; G.A.N. did bioinformatic analyses; L.V.W. confirmed ASC-dependent Dock2 expression in an independently generated line of ASC-deficient mice; D.R.G. contributed to the writing of the manuscript and conceptual insights; Y.F. provided reagents; T.-D.K., M.L., S.K.I., P.J.S., R.K.S.M., G.A.N. and Y.F. analyzed data; P.J.S., M.L. and T.-D.K. wrote the paper; and T.-D.K. conceived of the study, designed the experiments and provided overall direction.

COMPETING FINANCIAL INTERESTS

The authors declare no competing financial interests.

Published online at http://www.nature.com/natureimmunology/.
Reprints and permissions information is available online at http://www.nature.com/reprints/index.html.

1. Villani, A.C. *et al.* Common variants in the NLRP3 region contribute to Crohn's disease susceptibility. *Nat. Genet.* **41**, 71–76 (2009).
2. Zaki, M.H. *et al.* The NLRP3 inflammasome protects against loss of epithelial integrity and mortality during experimental colitis. *Immunity* **32**, 379–391 (2010).
3. Allen, I.C. *et al.* The NLRP3 inflammasome functions as a negative regulator of tumorigenesis during colitis-associated cancer. *J. Exp. Med.* **207**, 1045–1056 (2010).
4. Bauer, C. *et al.* Colitis induced in mice with dextran sulfate sodium (DSS) is mediated by the NLRP3 inflammasome. *Gut* **59**, 1192–1199 (2010).
5. Dupaul-Chicoine, J. *et al.* Control of intestinal homeostasis, colitis, and colitis-associated colorectal cancer by the inflammatory caspases. *Immunity* **32**, 367–378 (2010).
6. Jin, Y. *et al.* NALP1 in vitiligo-associated multiple autoimmune disease. *N. Engl. J. Med.* **356**, 1216–1225 (2007).
7. Martinon, F., Petrilli, V., Mayor, A., Tardivel, A. & Tschopp, J. Gout-associated uric acid crystals activate the NALP3 inflammasome. *Nature* **440**, 237–241 (2006).
8. Magitta, N.F. *et al.* A coding polymorphism in NALP1 confers risk for autoimmune Addison's disease and type 1 diabetes. *Genes Immun.* **10**, 120–124 (2009).
9. Larsen, C.M. *et al.* Interleukin-1-receptor antagonist in type 2 diabetes mellitus. *N. Engl. J. Med.* **356**, 1517–1526 (2007).
10. Agostini, L. *et al.* NALP3 forms an IL-1beta-processing inflammasome with increased activity in Muckle-Wells autoinflammatory disorder. *Immunity* **20**, 319–325 (2004).
11. Hoffman, H.M., Mueller, J.L., Broide, D.H., Wanderer, A.A. & Kolodner, R.D. Mutation of a new gene encoding a putative pyrin-like protein causes familial cold autoinflammatory syndrome and Muckle-Wells syndrome. *Nat. Genet.* **29**, 301–305 (2001).
12. Lamkanfi, M. Emerging inflammasome effector mechanisms. *Nat. Rev. Immunol.* **11**, 213–220 (2011).
13. Lamkanfi, M. & Dixit, V.M. The inflammasomes. *PLoS Pathog.* **5**, e1000510 (2009).
14. Lamkanfi, M. & Dixit, V.M. Inflammasomes: guardians of cytosolic sanctity. *Immunol. Rev.* **227**, 95–105 (2009).
15. Amer, A. *et al.* Regulation of Legionella phagosome maturation and infection through flagellin and host Ipaf. *J. Biol. Chem.* **281**, 35217–35223 (2006).
16. Franchi, L. *et al.* Cytosolic flagellin requires Ipaf for activation of caspase-1 and interleukin 1β in salmonella-infected macrophages. *Nat. Immunol.* **7**, 576–582 (2006).
17. Mariathasan, S. *et al.* Cryopyrin activates the inflammasome in response to toxins and ATP. *Nature* **440**, 228–232 (2006).
18. Miao, E.A. *et al.* Cytoplasmic flagellin activates caspase-1 and secretion of interleukin 1β via Ipaf. *Nat. Immunol.* **7**, 569–575 (2006).
19. Suzuki, T. *et al.* Differential regulation of caspase-1 activation, pyroptosis, and autophagy via Ipaf and ASC in Shigella-infected macrophages. *PLoS Pathog.* **3**, e111 (2007).
20. Sutterwala, F.S. *et al.* Immune recognition of *Pseudomonas aeruginosa* mediated by the IPAF/NLRC4 inflammasome. *J. Exp. Med.* **204**, 3235–3245 (2007).
21. Miao, E.A., Ernst, R.K., Dors, M., Mao, D.P. & Aderem, A. *Pseudomonas aeruginosa* activates caspase 1 through Ipaf. *Proc. Natl. Acad. Sci. USA* **105**, 2562–2567 (2008).
22. Franchi, L. *et al.* Critical role for Ipaf in *Pseudomonas aeruginosa*-induced caspase-1 activation. *Eur. J. Immunol.* **37**, 3030–3039 (2007).
23. Boyden, E.D. & Dietrich, W.F. Nalp1b controls mouse macrophage susceptibility to anthrax lethal toxin. *Nat. Genet.* **38**, 240–244 (2006).
24. Kanneganti, T.D. *et al.* Critical role for cryopyrin/Nalp3 in activation of caspase-1 in response to viral infection and double-stranded RNA. *J. Biol. Chem.* **281**, 36560–36568 (2006).
25. Sutterwala, F.S. *et al.* Critical role for NALP3/CIAS1/cryopyrin in innate and adaptive immunity through its regulation of caspase-1. *Immunity* **24**, 317–327 (2006).
26. Kanneganti, T.D. *et al.* Pannexin-1-mediated recognition of bacterial molecules activates the cryopyrin inflammasome independent of Toll-like receptor signaling. *Immunity* **26**, 433–443 (2007).
27. Muruve, D.A. *et al.* The inflammasome recognizes cytosolic microbial and host DNA and triggers an innate immune response. *Nature* **452**, 103–107 (2008).
28. Broz, P. *et al.* Redundant roles for inflammasome receptors NLRP3 and NLRC4 in host defense against Salmonella. *J. Exp. Med.* **207**, 1745–1755 (2010).
29. Wu, J., Fernandes-Alnemri, T. & Alnemri, E.S. Involvement of the AIM2, NLRC4, and NLRP3 inflammasomes in caspase-1 activation by *Listeria monocytogenes*. *J. Clin. Immunol.* **30**, 693–702 (2010).
30. Warren, S.E. *et al.* Cutting edge: cytosolic bacterial DNA activates the inflammasome via Aim2. *J. Immunol.* **185**, 818–821 (2010).
31. Tsuchiya, K. *et al.* Involvement of absent in melanoma 2 in inflammasome activation in macrophages infected with *Listeria monocytogenes*. *J. Immunol.* **185**, 1186–1195 (2010).
32. Sauer, J.D. *et al.* *Listeria monocytogenes* triggers AIM2-mediated pyroptosis upon infrequent bacteriolysis in the macrophage cytosol. *Cell Host Microbe* **7**, 412–419 (2010).
33. Rathinam, V.A. *et al.* The AIM2 inflammasome is essential for host defense against cytosolic bacteria and DNA viruses. *Nat. Immunol.* **11**, 395–402 (2010).
34. Fernandes-Alnemri, T. *et al.* The AIM2 inflammasome is critical for innate immunity to *Francisella tularensis*. *Nat. Immunol.* **11**, 385–393 (2010).
35. Miao, E.A. *et al.* Caspase-1-induced pyroptosis is an innate immune effector mechanism against intracellular bacteria. *Nat. Immunol.* **11**, 1136–1142 (2010).
36. Kanneganti, T.D., Lamkanfi, M. & Nunez, G. Intracellular NOD-like receptors in host defense and disease. *Immunity* **27**, 549–559 (2007).
37. Srinivasula, S.M. *et al.* The PYRIN-CARD protein ASC is an activating adaptor for caspase-1. *J. Biol. Chem.* **277**, 21119–21122 (2002).
38. Ellebedy, A.H. *et al.* Inflammasome-independent role of the apoptosis-associated speck-like protein containing CARD (ASC) in the adjuvant effect of MF59. *Proc. Natl. Acad. Sci. USA* **108**, 2927–2932 (2011).
39. McElvania Tekippe, E. *et al.* Granuloma formation and host defense in chronic Mycobacterium tuberculosis infection requires PYCARD/ASC but not NLRP3 or caspase-1. *PLoS ONE* **5**, e12320 (2010).
40. Ippagunta, S.K. *et al.* Inflammasome-independent role of apoptosis-associated speck-like protein containing a CARD (ASC) in T cell priming is critical for collagen-induced arthritis. *J. Biol. Chem.* **285**, 12454–12462 (2010).
41. Kolly, L. *et al.* Inflammatory role of ASC in antigen-induced arthritis is independent of caspase-1, NALP-3, and IPAF. *J. Immunol.* **183**, 4003–4012 (2009).
42. Shaw, P.J. *et al.* Cutting edge: critical role for PYCARD/ASC in the development of experimental autoimmune encephalomyelitis. *J. Immunol.* **184**, 4610–4614 (2010).
43. Trombetta, E.S. & Mellman, I. Cell biology of antigen processing in vitro and in vivo. *Annu. Rev. Immunol.* **23**, 975–1028 (2005).
44. Fukui, Y. *et al.* Haematopoietic cell-specific CDM family protein DOCK2 is essential for lymphocyte migration. *Nature* **412**, 826–831 (2001).
45. Mariathasan, S. *et al.* Differential activation of the inflammasome by caspase-1 adaptors ASC and Ipaf. *Nature* **430**, 213–218 (2004).
46. Sanui, T. *et al.* DOCK2 regulates Rac activation and cytoskeletal reorganization through interaction with ELMO1. *Blood* **102**, 2948–2950 (2003).
47. Gotoh, K. *et al.* Differential requirement for DOCK2 in migration of plasmacytoid dendritic cells versus myeloid dendritic cells. *Blood* **111**, 2973–2976 (2008).
48. Doherty, G.J. & McMahon, H.T. Mechanisms of endocytosis. *Annu. Rev. Biochem.* **78**, 857–902 (2009).
49. Kanneganti, T.D. Central roles of NLRs and inflammasomes in viral infection. *Nat. Rev. Immunol.* **10**, 688–698 (2010).
50. Taxman, D.J. *et al.* The NLR adaptor ASC/PYCARD regulates DUSP10, mitogen-activated protein kinase (MAPK), and chemokine induction independent of the inflammasome. *J. Biol. Chem.* **286**, 19605–19616 (2011).

ONLINE METHODS

Mice. Both independent *Asc*$^{-/-}$ mouse lines used in this study have been characterized[45,51]. *Nlrp3*$^{-/-}$, *Casp1*$^{-/-}$, *Tlr2*$^{-/-}$, *Tlr4*$^{-/-}$, *MyD88*$^{-/-}$, *Trif*$^{-/-}$ and *Dock2*$^{-/-}$ mice have been described[2,44]. All mice were backcrossed at least ten generations to the C57BL/6J genetic background. Mice were housed in a pathogen-free facility and animal studies were conducted under protocols approved by St. Jude Children's Research Hospital Committee on Use and Care of Animals or by the Ghent University Hospital ethical committee.

Microarray analysis and quantitative PCR. The quality of isolated RNA was confirmed with an Agilent 2100 Bioanalyzer before microarray analysis. RNA samples were processed on an HT MG-430 PM array plate with the Affymetrix GeneTitan system. Three biological replicates of naive wild-type and *Asc*$^{-/-}$ BMDCs were analyzed by microarray, and transcript expression values were summarized by the robust multi-array average method[52]. Differences between wild-type and *Asc*$^{-/-}$ BMDCs in gene expression were analyzed by an empirical Bayesian method (Cyber-T statistics program)[53], and the false-discovery rate was estimated as described[54]. For quantitative PCR analysis of *Dock2*, samples were amplified with specific primers (forward, 5′-TTGCTCAGCCAGCTACTGTATG-3′; reverse, 5′-TTGGTGATGACAGGAAGCAGAAT-3′). Quantification was normalized relative to expression of the reference gene *Gapdh*.

Subcellular fractionation. Cytoplasmic and nuclear fraction extractions were prepared with NE-PER Nuclear and Cytoplasmic Extraction Reagents according to the manufacturer's instructions (Pierce).

Immunoblot analysis. Standardized protein concentrations of cellular lysates were separated by SDS-PAGE. Antibody to Dock2 (anti-Dock2; 09-454), anti-ASC (AL177; Enzo Life Sciences), anti-caspase-1 (a gift from P. Vandenabeele), anti-FSTL1 (AF1738; R&D Systems), anti-FABP4 (2120; Cell Signaling Technology), anti-galanin (ab99452; Abcam) and anti-β-actin (4970; Cell Signaling Technology) were used at a final dilution of 1:1,000. Proteins were detected by horseradish peroxidase–based enhanced chemiluminescence (34095; Thermo Scientific).

Transfection. Immature BMDCs were transfected with a Nucleofector kit (VPA-1009; Lonza) and were incubated at 37 °C for 24 h before antigen-uptake assays.

Retroviral transduction. GFP-Dock2 and GFP were cloned into a mouse stem cell virus retroviral vector. Phoenix-Eco packaging cells were transfected with Lipofectamine 2000 (11668-027; Invitrogen), and recombinant viruses were collected 48 h and 72 h after transfection. Total spleen cells were isolated and cultured for 24 h with anti-CD3 (2.5 μg/ml; 145-2C11; eBioscience), anti-CD28 (5 μg/ml; 37.51; eBioscience) and IL-2 (100 U/ml) and then transduced with retrovirus by 'spin inoculation'. GFP$^+$ cells were sorted by flow cytometry and then used for chemotaxis assays.

T cell proliferation. Popliteal lymph nodes were collected 10 d after immunization with 10 μg BSA (Sigma, 85040) in complete Freund's adjuvant emulsion. CD4$^+$ T cells were isolated by negative selection by a mouse CD4$^+$ T cell–enrichment strategy (AutoMACS; 130-095-248; Milteny). CD4$^+$CD11c$^+$ DCs (130-091-262) were isolated from spleens of naive wild-type and *Asc*$^{-/-}$ mice treated with collagenase-D (11088874103) according to the manufacturer's instructions (Roche). Cocultures were started with 5×10^5 CD4$^+$ T cells per well and 2.5×10^5 DCs per well and the appropriate concentration of antigen. Cultures were maintained for 72 h at 37 °C and 5% CO2 in U-bottomed plates in 300 μl HL-1 medium (7720; Lonza) supplemented with penicillin G (50 U/ml) and streptomycin (50 μg/ml), 2-mercaptoethanol (50 μM), L-glutamine (292 μg/ml) and 0.1% (wt/vol) BSA. Supernatants were collected for evaluation of cytokine production and cultures were pulsed with [^{3}H]thymidine (1 μCi/well in 10 μl), then were incubated for an additional 18 h and collected onto UniFilter GF/C plates, then radioactivity was measured as counts per minute on a TopCount NXT microplate scintillation counter (PerkinElmer).

Cytokine measurement. Cytokines were measured with a Milliplex ELISA kit (Millipore).

Flow cytometry. For flow cytometry, cells were stained with anti-CD4 (L3T4), anti-CD8 (53-6.7), anti-CD11b (M1/70) or anti-B220 (RA3-6B2; all from eBioscience); or anti-CD8α (53-6.7), anti-TCRβ (H57-597), anti-CD44 (IM7), anti-CD69 (H1.2F3), anti-CD11c (N418), anti-CD45.1 (A20) or anti-CD45.2 (104; all from Biolegend); after staining, cells were analyzed on an LSR II (Becton-Dickinson). For analysis of antigen uptake and phagocytosis, DCs were incubated for 3 h with fluorochrome-conjugated OVA, dextran, luciferase yellow, zymosan A or beads. Cells were washed several times and analyzed by flow cytometry. For analysis of actin polymerization, isolated T cells and B cells were fixed in 4% (vol/vol) paraformaldehyde, made permeable with Permeabilization Wash Buffer (421002; Biolegend) and stained with Alexa Fluor 488–labeled phalloidin (BD Biosciences) for flow cytometry.

Confocal microscopy. BMDCs (1×10^5) were plated on glass cover slips (BD Biosciences) and, 24 h later, cells were stimulated, washed in PBS and fixed for 10 min in 4% (vol/vol) paraformaldehyde. Cells were made permeable for 5 min with 0.1% (vol/vol) Triton X-100. Blockade was achieved by incubation for 60 min with blocking buffer (1% (vol/vol) BSA in PBS and 0.1% (vol/vol) Triton X-100). Cells were stained for 1 h with mouse monoclonal anti-ASC (1 μg/ml; 04-147; Millipore) and rabbit polyclonal antibody to caspase-1 (ref. 51; a gift from P. Vandenabeele) in blocking buffer. After cells were washed, bound antibodies were detected for 1 h at 25 °C with Alexa Fluor 488–conjugated goat anti-rabbit (for caspase-1 (green); A-11034; Molecular probes) and Alexa Fluor 647–conjugated chicken anti-mouse (for ASC (red); A-21463; Molecular probes). Slides were mounted with ProLong Gold-DAPI mounting media (P-36931; Invitrogen) and were analyzed with an inverted spinning-disk confocal microscope (Zeiss) with a 63× objective lens with Slidebook software. The specificity of anti-ASC and anti-caspase-1 was confirmed through the use of *Asc*$^{-/-}$ and *Casp1*$^{-/-}$ BMDCs, respectively, as a negative control.

Luciferase (promoter activity) assay. The *Dock2* promoter (positions −3931 to +132) was amplified from mouse genomic DNA (forward primer, 5′-GATCGTCGACGCAAGGTCAGAAATTTTGTTAGAAAAGATTTTAAA-3′; reverse primer, 5′-CATGGGATCCCCCACACTTGCCCACACCTAC-3′) and was cloned in to the pGL3-Enhancer vector upstream to the firefly luciferase reporter gene. BMDCs were transfected with combinations of the pGL3-Enhancer–*Dock2* promoter reporter plasmid or pGL3-Enhancer empty vector and control renilla luciferase plasmid (pTK-RL) through the use of an Amaxa DC Nucleofector kit (Lonza). Luciferase activity was quantified 24 h after transfection with the Dual-Luciferase Reporter Assay System according to the manufacturer's instructions (Promega). *Dock2* promoter activity (firefly luciferase) was normalized to the internal control (renilla luciferase).

Competitive-reconstitution mixed chimeras. Wild-type CD45.1$^+$ congenic mice were lethally irradiated with a split dose of 1,200 rads. Bone marrow from CD45.1$^+$CD45.2$^+$ wild-type mice and CD45.2$^+$*Asc*$^{-/-}$ mice was injected intravenously at a ratio of 1:1. After 6 weeks of reconstitution, the frequency of wild-type and *Asc*$^{-/-}$ CD4$^+$ T cells and B cells was calculated with anti-CD45.1 (A20; Biolegend) and anti-CD45.2 (104; Biolegend).

Chemotaxis assay. Splenocytes (1.5×10^6) in 100 μl RPMI medium were placed in Transwell permeable supports (pore size, 5 μm), which were placed onto 24-well plates containing 500 μl RPMI medium supplemented with chemokines (R&D Systems) at various concentrations. Cells were incubated for 3 h at 37 °C. Cells placed in the Transwell supports and those that migrated to the lower chamber were collected and stained with anti-TCRβ (H57-597; eBioscience) and anti-B220 (RA3-6B2; eBioscience).

GTPase activity assay. The GTPase activity of Cdc42 and Rac1 in cell extracts was measured by G-LISA activation assay (BK127 (for Cdc42) and BK127 (for Rac1); Cytoskeleton).

Assay of mRNA stability. New transcription was inhibited by culture of BMDCs in the presence of DRB (5,6-dichloro-1-β-ribofuranosyl

benzamidazole; 50 μM; D191; Sigma-Aldrich) or actinomycin D (5 μg/ml; A1410; Sigma-Aldrich). Total RNA was then isolated for measurement of the abundance of *Dock2* and *Actb* transcripts by real-time quantitative RT-PCR. Transcript abundance was normalized to that of *Gapdh*.

Statistical analysis. *P* values were calculated with Student's *t*-test. *P* values of less than 0.05 were considered significant.

51. Kanneganti, T.D. *et al.* Bacterial RNA and small antiviral compounds activate caspase-1 through cryopyrin/Nalp3. *Nature* **440**, 233–236 (2006).
52. Irizarry, R.A. *et al.* Exploration, normalization, and summaries of high density oligonucleotide array probe level data. *Biostatistics* **4**, 249–264 (2003).
53. Baldi, P. & Long, A.D. A Bayesian framework for the analysis of microarray expression data: regularized t-test and statistical inferences of gene changes. *Bioinformatics* **17**, 509–519 (2001).
54. Benjamini, Y. & Hochberg, Y. Controlling the false discovery rate: a practical and powerful approach to multiple testing. *J.R. Stat. Soc. B* **57**, 289–300 (1995).

doi:10.1038/ni.2095

Addendum: Defective Dock2 expression in a subset of ASC-deficient mouse lines

Sirish K Ippagunta[1,7], R K Subbarao Malireddi[1,7], Patrick J Shaw[1,7], Geoffrey A Neale[2], Lieselotte Vande Walle[3,4], Yoshinori Fukui[5,6], Douglas R Green[1], Mohamed Lamkanfi[3,4] & Thirumala-Devi Kanneganti[1]

[1]Department of Immunology St. Jude Children's Research Hospital, Memphis, Tennessee, USA. [2]Hartwell Center for Bioinformatics and Biotechnology, St. Jude Children's Research Hospital, Memphis, Tennessee, USA. [3]Department of Biochemistry, Ghent University, Ghent, Belgium. [4]Department of Medical Protein Research, VIB, Ghent, Belgium. [5]Division of Immunogenetics, Kyushu University, Kyushu, Japan. [6]Department of Immunobiology and Neuroscience Medical Institute of Bioregulation, Kyushu University, Kyushu, Japan. [7]These authors contributed equally to this work. Correspondence should be addressed to M.L. (mohamed.lamkanfi@vib-ugent.be) or T.-D.K. (thirumala-devi.kanneganti@stjude.org).

Published reports suggest that the inflammasome adaptor ASC regulates immune responses independently of its well-known role in inflammasomes. In this context, ASC-deficient mice (*Pycard*$^{-/-}$ mice; called '*Asc*$^{-/-}$ mice' here) have been found to be resistant to antigen- and collagen-induced arthritis and experimental autoimmune encephalomyelitis, but mice deficient in the cytoplasmic receptor NLRP3 (*Nlrp3*$^{-/-}$ mice) or caspase-1 (*Casp1*$^{-/-}$; as noted below, these mice are actually doubly deficient in caspase-1 and caspase-11)[1] are not[2–4]. In addition, granuloma formation and host defense during chronic infection with *Mycobacterium tuberculosis* has been suggested to require ASC but not NLRP3 or caspase-1 (ref. 1). In our article, we reported defective expression of the guanine nucleotide–exchange factor Dock2 in the bone marrow–derived macrophages (BMDMs), bone marrow–derived dendritic cells (BMDCs), T cells and B cells of mice with targeted deletion of *Asc*[5], thereby providing a possible explanation for the previously reported defects in antigen presentation and lymphocyte migration in these mice[4]. In this context, Dock2 has already been established as a central regulator of the migration of lymphocytes and plasmacytoid dendritic cells[6–8]. In addition, we demonstrated defective antigen uptake in Dock2-deficient BMDCs similar to that of ASC-deficient cells and that ectopic expression of Dock2 in ASC-deficient BMDCs and lymphocytes restored antigen uptake and lymphocyte migration, respectively[5].

In our facility, we have specifically observed defective Dock2 expression in *Asc*$^{-/-}$ mice, but not in mice deficient in the kinase RICK (*Ripk2*$^{-/-}$ mice), the cytosolic pattern-recognition receptor Nod2 (*Nod2*$^{-/-}$ mice), the adaptors CARD9 (*Card9*$^{-/-}$ mice), TRIF (*Ticam1*$^{-/-}$ mice; called '*Trif*$^{-/-}$ mice' here) or MyD88 (*Myd88*$^{-/-}$ mice), the cytosolic pattern-recognition receptors Nod1 and Nod2 (*Nod1*$^{-/-}$*Nod2*$^{-/-}$ mice), the signaling adaptor MAVS (*Mavs*$^{-/-}$ mice), or the pattern-recognition receptor NLRC4 (*Nlrc4*$^{-/-}$ mice) or in *Nlrp3*$^{-/-}$ mice (**Fig. 1a**). Moreover, defective Dock2 expression has been verified in BMDMs and BMDCs from two independently generated lines of ASC-deficient mice housed in two separate facilities (St Jude Children's Research Hospital, Memphis, Tennessee, USA, and Ghent University, Ghent, Belgium)[5], which makes it unlikely that this is a strain-specific anomaly. The two lines of ASC-deficient mice available to us were generated through the use of embryonic stem cells from mice of the 129 strain[9,10]. Notably, a published study has shown that *Casp1*$^{-/-}$ mice also lack caspase-11 expression because of a mutation in the locus encoding caspase-11 (*Casp4*; called '*Casp11*' here) in the 129 embryonic stem cells used to generate these mice[11]. However, unlike the *Casp1* and *Casp11* loci, the *Asc* and *Dock2* loci reside on separate chromosomes. Moreover, genome-wide single-nucleotide polymorphism (SNP) analysis has confirmed that both of our ASC-deficient mouse lines are approximately 98% identical to C57BL/6 mice (**Fig. 1b**). In addition, we have found normal expression of Dock2 in BMDCs of C57BL/6, 129S1/SvImJ and BALB/c mice (**Fig. 1c**), which suggests that the defective Dock2 expression in these ASC-deficient mice cannot be attributed to their overall genetic background. However, when we examined Dock2 expression in *Asc*$^{-/-}$ mice from other investigators' facilities, we unexpectedly observed defective Dock2 expression in BMDCs and BMDMs of some, but not all, ASC-deficient mouse lines (**Fig. 1d**,**e**).

As our results were highly reproducible, we believe the most probable explanation for the differences in Dock2 expression in different ASC-deficient lines may be subtle differences in genetic background and/or environmental factors. In this context, *Asc*$^{-/-}$ mice have been shown to harbor an altered microflora composition, which leads to the development of a severe dextran sodium sulfate–induced colitis that is transferable to wild-type mice housed together with newborn *Asc*$^{-/-}$ mice that were cross-fostered at birth with wild-type mothers[12]. Alternatively, ASC-deficient mouse lines that fail to express Dock2 may be hemi- or homozygous for an inactivating 'passenger' mutation of *Dock2*. In this context, a spontaneous genomic duplication and frameshift mutation in *Dock2* that reaches homozygosity has been reported to complicate the interpretation of interferon and antibody responses in at least a subset of available mice deficient in the transcription factor IRF5 (ref. 13). Further analysis is warranted, although sequencing of PCR-amplified *Dock2* cDNA isolated from ASC-deficient macrophages with lower Dock2 expression (lines 1 and 2) has failed to identify any missense mutations in *Dock2* (**Fig. 1f**).

In conclusion, the precise reasons for the differences in Dock2 expression in some, but not all, ASC-deficient mouse lines remain unclear and should be explored further in future experiments. Nevertheless, our new experimental data emphasize the proposal that verifying the Dock2-expression status of the various ASC-deficient mouse lines now available is imperative for proper determination and interpretation of the inflammasome-dependent and inflammasome-independent phenotypes of these mice.

ACKNOWLEDGMENTS

We thank R. Flavell (Yale University School of Medicine), G. Nunez (University of Michigan), S. Akira (Osaka University) and V. Dixit (Genentech) for mutant mice, and A. Amer (Ohio State University) and K. Fitzgerald (University of Massachusetts) for femurs from *Asc*$^{-/-}$ mouse lines.

1. McElvania Tekippe, E. *et al.* Granuloma formation and host defense in chronic Mycobacterium tuberculosis infection requires PYCARD/ASC but not NLRP3 or caspase-1. *PLoS ONE* **5**, e12320 (2010).
2. Kolly, L. *et al.* Inflammatory role of ASC in antigen-induced arthritis is independent of caspase-1, NALP-3, and IPAF. *J. Immunol.* **183**, 4003–4012 (2009).
3. Ippagunta, S.K. *et al.* Inflammasome-independent role of apoptosis-associated speck-like protein containing a CARD (ASC) in T cell priming is critical for collagen-induced arthritis. *J. Biol. Chem.* **285**, 12454–12462 (2010).
4. Shaw, P.J. *et al.* Cutting edge: critical role for PYCARD/ASC in the development of experimental autoimmune encephalomyelitis. *J. Immunol.* **184**, 4610–4614 (2010).

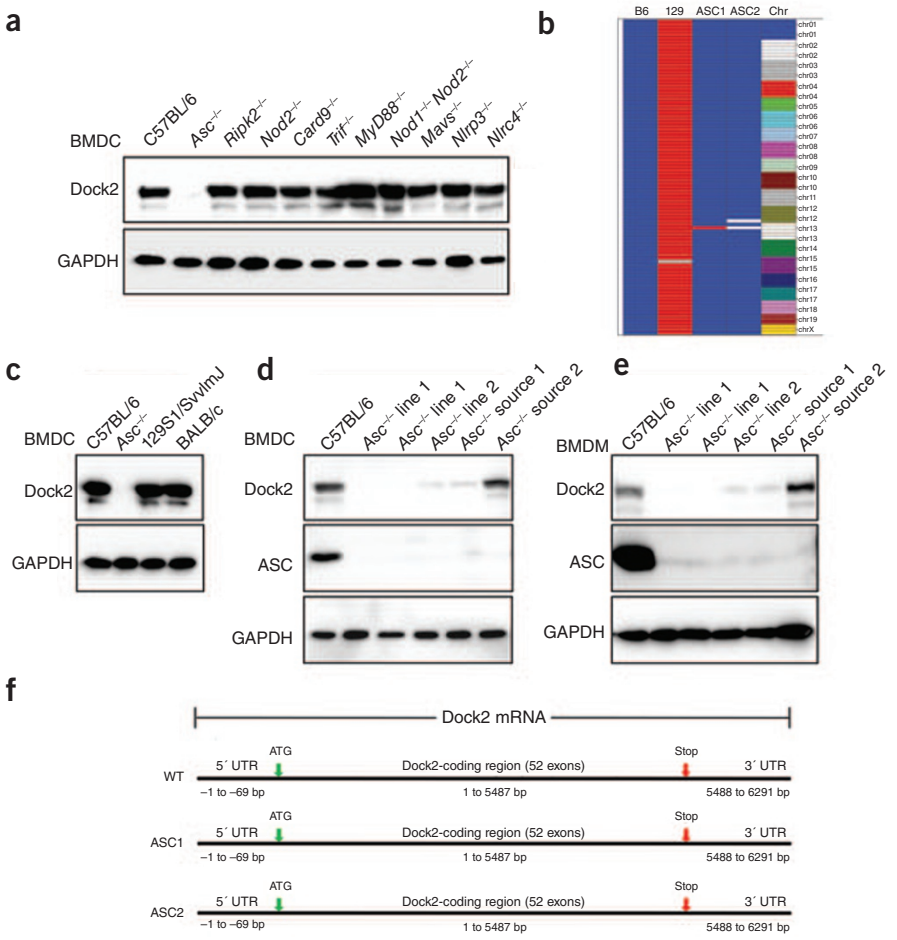

Figure 1 Dock2 expression in BMDCs and BMDMs. (**a**) Immunoblot analysis of Dock2 in lysates of BMDCs from wild-type (C57BL/6) and mutant mice (genotypes above lanes). GAPDH (glyceraldehyde phosphate dehydrogenase) serves as a loading control throughout. (**b**) Genome-wide SNP analysis of mouse strains ASC1 (St Jude Children's Research Hospital; original source, Millennium Pharmaceuticals) and ASC2 (Ghent University; original source, Genentech), which are 98.9% identical (ASC1) and 97.8% identical (ASC2) to the C57BL/6J (B6) strain. Blue indicates homozygous C57Bl/6J genotype; red indicates 129S1/SvImJ genotype; white indicates heterozygous genotype between strains; gray indicates 'no call' at that position in the genome. Far right, chromosome location(Chr) of SNPs investigated. Heterozygous and homozygous SNPs associated with the 129S1/SvImJ (129) strain are present only on chromosomes 12 and 13. (**c**) Immunoblot analysis of Dock2 in naive BMDCs from C57BL/6, *Asc*$^{-/-}$, 129S1/SvImJ and BALB/c mice. (**d**,**e**) Immunoblot analysis of Dock2 in BMDCs (**d**) and BMDMs (**e**) from wild-type mice and *Asc*$^{-/-}$ mice from the following facilities: line 1, St Jude Children's Research Hospital; line 2, Ghent University; source 1, Ohio State University; source 2, University of Massachusetts Medical School. (**f**) Sequence analysis of Dock2 cDNA in BMDMs from *Asc*$^{-/-}$ mouse lines 1 and 2. Data are representative of three independent experiments.

5. Ippagunta, S.K. *et al.* The inflammasome adaptor ASC regulates the function of adaptive immune cells by controlling Dock2-mediated Rac activation and actin polymerization. *Nat. Immunol.* **12**, 1010–1016 (2011).
6. Fukui, Y. et al. Haematopoietic cell-specific CDM family protein DOCK2 is essential for lymphocyte migration. Nature 412, 826–831 (2001).
7. Sanui, T. et al. DOCK2 regulates Rac activation and cytoskeletal reorganization through interaction with ELMO1. Blood 102, 2948-2950 (2003).
8. Gotoh, K. *et al.* Differential requirement for DOCK2 in migration of plasmacytoid dendritic cells versus myeloid dendritic cells. *Blood* **111**, 2973-2976 (2008).
9. Mariathasan, S. *et al.* Differential activation of the inflammasome by caspase-1 adaptors ASC and Ipaf. *Nature* **430**, 213–218 (2004).
10. Ozören, N. *et al.* Distinct roles of TLR2 and the adaptor ASC in IL-1β/IL-18 secretion in response to Listeria monocytogenes. *J. Immunol.* **176**, 4337–4342 (2006).
11. Kayagaki, N. *et al.* Non-canonical inflammasome activation targets caspase-11. *Nature* **479,** 117-121 (2011).
12. Elinav, E. *et al.* NLRP6 inflammasome regulates colonic microbial ecology and risk for colitis. *Cell* **145**, 745–757 (2011).
13. Purtha, W.E., Swiecki, M., Colonna, M., Diamond, M.S. & Bhattacharya, D. Spontaneous mutation of the Dock2 gene in Irf5–/– mice complicates interpretation of type I interferon production and antibody responses. *Proc. Natl. Acad. Sci. USA* 109, E898-E904 (2012).
14. Kobayashi, K. *et al.* RICK/Rip2/CARDIAK mediates signalling for receptors of the innate and adaptive immune systems. *Nature* **416**, 194–199 (2002).
15. Kobayashi, K.S. *et al.* Nod2-dependent regulation of innate and adaptive immunity in the intestinal tract. *Science* **307**, 731–734 (2005).
16. Zaki, M.H. *et al.* The NLRP3 inflammasome protects against loss of epithelial integrity and mortality during experimental colitis. *Immunity* **32**, 379–391 (2010).
17. Kanneganti, T.D. *et al.* Bacterial RNA and small antiviral compounds activate caspase-1 through cryopyrin/Nalp3. *Nature* **440**, 233–236 (2006).
18. Chamaillard, M. *et al.* An essential role for NOD1 in host recognition of bacterial peptidoglycan containing diaminopimelic acid. *Nat. Immunol.* **4**, 702–707 (2003).
19. Hsu, Y.M. *et al.* The adaptor protein CARD9 is required for innate immune responses to intracellular pathogens. *Nat. Immunol.* **8**, 198–205 (2007).
20. Kumar, H. *et al.* Essential role of IPS-1 in innate immune responses against RNA viruses. *J. Exp. Med.* **203**, 1795–1803 (2006).
21. Hornung, V. *et al.* AIM2 recognizes cytosolic dsDNA and forms a caspase-1-activating inflammasome with ASC. *Nature* **458**, 514–518 (2009).

METHODS

Mice.
The *Ripk2*$^{-/-}$, *Nod2*$^{-/-}$, *Card9*$^{-/-}$, *Trif*$^{-/-}$, *Myd88*$^{-/-}$, *Nod1*$^{-/-}$*Nod2*$^{-/-}$, *Mavs*$^{-/-}$, *Nlrp3*$^{-/-}$ and *Nlrc4*$^{-/-}$ mice and the four *Asc*$^{-/-}$ mouse lines have been reported before[14–21]. Mice were housed in a pathogen-free facility and animal studies were done according to protocols approved by St. Jude Children's Research Hospital Committee on Use and Care of Animals.

Generation of BMDCs.
Bone marrow cells isolated from femurs of 6- to 12-week-old mice were cultured for 7 d at 37 °C in RPMI medium containing 10% heat-inactivated FBS, 100 μM 2-mercaptoethanol, 100 U/ml penicillin and 100 μg/ml of streptomycin, supplemented with granulocyte-macrophage colony-stimulating factor (20 ng/ml), in a humidified atmosphere containing 5% CO_2. On days 3 and 5, half of the medium was replaced with fresh medium containing 40 ng/ml granulocyte-macrophage colony-stimulating factor. Lysates were prepared on day 7 for immunoblot analysis.

Generation of BMDMs.
Bone marrow isolated from the femurs of 6- to 12-week-old mice was cultured at 37 °C in Iscove's modified Dulbecco's medium containing 10% heat-inactivated FBS, 20% conditioned medium from L cells (mouse fibroblasts lacking thymidine kinase), 100 U/ml of penicillin, and 100 μg/ml of streptomycin, in a humidified atmosphere containing 5% CO_2. After 5–7 d of incubation, cells were collected and plated in six-well plates in Iscove's modified Dulbecco's medium containing 10% heat-inactivated FBS and antibiotics. Macrophages were cultured for an additional 24 h before lysates were prepared for immunoblot analysis.

Immunoblot analysis.
Standardized protein concentrations of cellular lysates were separated by SDS-PAGE. Antibody to Dock2 (09-454; Millipore), to ASC (AL177; Enzo Life Sciences) and to β-actin (4970; Cell Signaling Technology) were used at a final dilution of 1:1,000. Proteins were detected by horseradish peroxidase–based enhanced chemiluminescence (34095; Thermo Scientific).

Genome-wide SNP analysis.
SNPs were assayed through the use of a panel of 93 custom-designed SNPs (median intermarker distance of 22.2 megabases; five markers per chromosome) that discriminate between the C57BL/6J and 129S1/SvImJ mouse strains. DNA from mouse tails was assayed with the Illumina GoldenGate assay on the BeadXpress system according to the manufacturer's recommended procedures (Illumina).

RT-PCR and sequencing.
Total RNA was isolated from the BMDCs with TRIzol RNA-extraction reagent (Invitrogen). Full-length *Dock2* cDNA was amplified from 500 ng total RNA with gene-specific primers (forward, 5′-AAGGCGCCTAACCACCCCAGCCA-3′; reverse, 5′-GGTATCATTTCAAATTGTGCTATCATTCC-3′) and the SuperScript III One-Step RT-PCR System with Platinum Taq (Invitrogen). The *Dock2* cDNA sequence was analyzed by the Sanger dideoxy sequencing method.